JCEC
THE JOURNAL OF ENGINEERING AND EXACT SCIENCES

OPEN ACCESS

The Journal of Engineering and Exact Sciences – jCEC, Vol. 09 N. 07 (2023)
journal homepage: https://periodicos.ufv.br/jcec
eISSN: 2527-1075
ISSN: 2446-9416

Application of rice shell activated carbon for reduction of chemical oxygen demand limit and adsorption of iron from abattoir wastewater

Article Info:
Article history: Received 2023-01-06 / Accepted 2023-04-01 / Available online 2023-04-11
doi: 10.18540/jcecvl9iss7pp15621-01e

Robinson David Udo
ORCID: https://orcid.org/0000-0003-0701-9858
Federal University of Technology Minna, Nigeria
E-mail: robinsondavid357@gmail.com
Samuel Ayegu Tsebam
ORCID: https://orcid.org/0009-0001-4085-8218
Federal University of Technology Minna, Nigeria
E-mail: tsebamsamuel@gmail.com
Kolade Olawale Samson
ORCID: https://orcid.org/00000-0002-9957-8798
King Fahd University of Petroleum and Minerals, Saudi Arabia
E-mail: olawale.kolade.2016@gmail.com
Precious Nya Umo
ORCID: https://orcid.org/0009-0001-4085-8218
University of Calabar, Nigeria
E-mail: preciousumo3@gmail.com
Lawal Solomon Adeniyi
ORCID: https://orcid.org/0009-0005-0886-5871
Federal University of Petroleum Resources Effurun, Nigeria
E-mail: figaroperfect@gmail.com
Juliet Gordon
ORCID: https://orcid.org/0009-0001-2401-3370
Federal University of Technology Minna, Nigeria
E-mail: gordonjuliet571@gmail.com
Oluwaseun Fetuata
ORCID: https://orcid.org/0009-0005-8896-4975
Obafemi Awolowo University, Nigeria
E-mail: fetuataoluwaseun@gmail.com
Ibrahim Ademola Fetuga
ORCID: https://orcid.org/0000-0002-1943-4234
University of Lagos, Nigeria
E-mail: fetugaebraheem@gmail.com
Olabode Thomas Olakoyejo
ORCID: https://orcid.org/0000-0001-9942-1339
University of Lagos, Nigeria
E-mail: oolakoyejo@unilag.edu.ng
Antônio Marcos de Oliveira Siqueira
ORCID: https://orcid.org/0000-0002-7088-3211
Federal University of Viçosa, Brazil
E-mail: antonio.siqueira@ufv.br

Abstract
In this investigation, rice shell (RS)-activated carbon (AC) - (RS-AC) is used as a bio-sorbent to reduce chemical oxygen demand (COD) and adsorb iron from effluent from an abattoir. With H_3PO_4, the rice husk was altered and chemically activated. Scan electron microscopy (SEM) as well as Fourier-Transform-Infrared (F-T-IR) were utilized to examine the activated RS and examine its content, appearance, and structure. Moreover, proximate analytical study was used to ascertain the activated rice husk's wetness, volatile matter, ash, bulk density, and fixed carbon contents. Contact period, temperature, and dosage are the adsorption parameters that are assessed. The contact period of 10, 20, 30, 40, 50, and 60 min, the dosage of 0.1, 0.2, 0.3, 0.4, 0.5, and 0.6g, and the temperature of 20, 40, 60, 80, and 100^{o}C were evaluated for the Fe bio-adsorption as well as COD limits reduction in wastewater obtained from abattoir at constant agitation of 200rmp and potential hydrogen level of 5 for all the runs. RS-AC can be used to maintain the amount of iron and COD in aqueous solutions and water treatment, according to the results. According to this investigation, ARH has a high fixed carbon content, which makes it an efficient bio-adsorbent, and the resulting RS-AC has a good bulk density for flow consistency. The FI-M best matches the linear equation for iron removal, whereas the LI-M given that the coefficient of correlation that well matches the equation to have COD limit at acceptable level. In comparison to other models, second ordered Kinetics model-SOKM satisfactorily describes current data to keep Fe as well as COD levels within standard ranges; as a result, chemical adsorption controls the bio-adsorption process.
Keywords: RS-AC. Iron. COD. Adsorption. Isotherms. Kinetic models.

Nomenclature

$A_{.C}$	*Ash Content*
AC	*Activated Carbon*
ARH	*Activated Rice Husk*
ASTM	*American Society for Testing and Materials*
COD	*Chemical Oxygen Demand*
DO	*Dissolved Oxygen*
EKM	*Elovich Kinetic Model*
$F_{.C}$	*Fixed Carbon Content*
Fe	*Iron*
FI-M	*Freundlich Isotherm Model*
FTIR	*Fourier Transform Infrared*
LI-M	*Langmuir Isotherm Model*
$M_{.C}$	*Moisture Content*
PFOKM	*Pseudo First Order Kinetic Model*
RS	*Rice Shell*
RS-AC	*Rice shell Activated Carbon*
SEM	*Scan Electron Microscopy*
SOKM	*Second Order Kinetic Model*
$V_{.M}$	*Volatile Moisture Content*

1. Introduction

Organic waste from abattoir operations contains considerable amounts of suspended hard fluid and fat. Rejected food, food products containing cellular debris, dentures, hair, bones, horns, and aborted babies are some of the solid wastes. Liquid waste often includes dissolved substances, perspiration, liver, feces, and liquid waste (Adeyemi & Asubmissio, 2007). Animal waste is frequently carried into rivers, endangering aquatic life and the safety of water used for residential purposes. The environment, people, and animals are all affected differently by high COD and iron (Fe) limits in abattoir wastewater. Higher limits of COD as well as Fe may contribute to a number

of negative effects, including the extinction of marine life, aquifer depletion, and occasionally, a risky influence on living things, as biological supplements linked to liquid tables end up increasing bacteria loads, leading to unfavorable sea preferences and odors, which may, in fact, contribute to a number of negative impacts, such as the decline of undersea life, the value of aquifers, and maybe, adverse effects on living things (Mekuria *et al.*, 2021). High COD limits lead to a greater need for oxygen, which implies that the water body has more oxidizable organic compounds and lower levels of dissolved oxygen (DO).

When hazardous chromium is removed from aqueous solutions while keeping COD limits, carbonized rice shell beads made from a mixture of Fe (metal) and carbonized rice shell are an efficient bio-adsorbent. The results showed that 2.0 was the ideal potential hydrogen level for removing Cr (VI) ions, which was significantly reliant on the adsorption towards Chromium ions (Sugashini *et al.*, 2013). Bio-adsorption of Pb(II) from aqueous-solution, AC (carbon activated) with a high surface area is prepared using rice shell, a byproduct of agricultural activities. The porosity and surface chemistry of the carbon sample were related to its adsorption capability. As the carbon was oxidized, lead adsorption increased significantly, proving that coordination with surface active group(s) had significance in lead adsorption. Studies shows clearly that potential hydrogen level of the substance had a significant impact on the bio-adsorption, with potential hydrogen level of 5 producing the highest quantity adsorbed (Vassileva *et al.*, 2013). To extract Cr (VI) from aqueous solutions, rice shells were reacted with sulfuric acid giving a carbon-bio-adsorbent. According to the study, total chromium adsorption followed a SOKM while Cr-(VI) ion elimination towards potential hydrogen level of 2 modeled the first kinetic model pattern. Greatest amount of Chromium (iii) ions was absorbed resulting from of Chromium (vi) ion decrease and an increase in solution potential hydrogen level. So, it is possible to interpret the surface-adsorption of chromium(vi)-ions onto a bio-adsorbent signifying a sign of reduction-bio-adsorption processes (El-Shafey *et al.*, 2005).

Thus, it is necessary to lower the COD limit, which is to blame for raising the DO in wastewater prior to discharge. Leaks or spills from sewage treatment plants may be brought on by high potential hydrogen level in the water resulting to the water's rust-red color and metallic taste and odor are caused by Fe, which also has other negative effects like bacterial development in pipes and itching skin (Aniyikaiye *et al.*, 2019). As a result, maintaining appropriate COD and Fe levels in wastewater is required before disposal.

Therefore, this study investigated the utilization of AC made from RS to preserve the COD and Fe limitations through bio-adsorption in abattoir effluent from a slaughterhouse in Nigeria.

2. Materials used and methodology

2.1 Sampling-processing of samples

Federal University of Technology Minna Gidan kwano off-campus local rice millers in Niger State, Nigeria, where the rice shell (RS) was collected. The indigenous rice millers close to Gidan Kwano main campus, in Niger State, Nigeria, provided rice shell for the research studies. The shell underwent a four-day process of sun drying after being cleaned with water to eliminate dirt and grimes. The sample's mass was obtained and recorded (Zhang *et al.*, 2019).

2.2 Chemical modification of RS-AC

To get rid of the surfactant, the RS was additionally washed with distillate water. The sample was de-moisturised: once at a temperature equivalent to that of a room and additional drying using an oven set at 110°C. It was weighed continuously till a consistent mass was obtained continuously via the weighing process. The obtained RS-treated was continuously stirred in 0.5M H_3P0_4 (maintaining 60ºC) for period of 30min after washing. The RS was additional washed with distillate water to discard any remaining acids, filtered, and allowed to air dry once the acid solution had been removed. The rice shell was then further dried in a 110°C oven for 2hr. To create rice shell AC, the

carbonized sample was oven-calcined at 400°C, one hour and 10°C/min rate. The grand percentage yielded product and carbon burn-off of the AC produced from RS were determined using equations 1 and 2.

$$Percentage\ yield = \frac{100 \times S_1}{S_o}\% \quad (1)$$

$$Percentage\ burn\ off = \frac{100 \times S_2}{S_o}\ \% \quad (2)$$

Noted that S_o is previous mass of the de-moisturised sample, [g], S_1 is the new mass of dried RS-AC, [g] and S_2 is the weighted mass of burnt-off sample after combustion [g].

2.3 Wastewater Preparation

A wastewater specimen was taken from the abattoir in Minna city (tayi hamlet) and analyzed for pollutants.

2.4 RS-AC Characterization

The RS-AC's wetness content, volatile matter, bulk density, fixed carbon content, and ash content were all determined using proximate analytical studies. The determination of the distribution of products produced when the carbon sample is heated under specific circumstances is known as the proximate analytical studies of a material. According to ASTM (D-121), proximate analytical studies divide the end products into four categories: wetness, volatile matter (which consists gaseous vapour pushed away on pyrolytic process), fixed amount of carbon content, and amount of ash content (inorganic clog left after burn-off). Most popular technique for characterizing a material in relation to its use is proximate analytical studies. The precursor's proximate analytical studies were performed using methods that adhere to ASTM-standards. SEM and FTIR examination revealed the morphology potential and functional grouping of the rice shell AC.

Determination of wetness content: After measuring 200g of the sample weight, it was put in a crucible with a known weight. It was evenly distributed across the crucible. It was then dried to a consistent weight while being baked in an oven at 105ºC. The crucible was not covered throughout the heating process or was left uncovered. Following heating, the crucible was taken out and allowed to cool to room temperature before the finished product was weighed and recorded. The same process was carried out three times, with the average value serving as the wetness content measurement. Afterwards, Equation 3 was used to get the percentage wetness content.

$$Percentage\ of\ M._c = \frac{100 \times (C-G)}{C-H} \quad (3)$$

Note that C is the crucible mass, [g] + sample mass before subjecting to heating, [g], G is the crucible mass, [g] + sample mass after the heating process, [g], H is the mass of the crucible (empty) and $M._C$ is wetness content, [%].

Determination of volatile matter: When the wetness was removed, 190g of the sample was transferred into a known mass crucible, lid covered and heated up in a muffle furnace for precisely one hour at 300ºC. The crucible was then weighted and desiccated to cool it. The same process was carried out three times, with the average value serving as the volatile matter value. Then, using Equation 4, the percentage of volatile content of matter on a dry basis is determined.

$$Percentage\ V._M = \frac{100 \times \{100(C-G) - M._c(C-H)\}}{(C-H)(100 - M._c)} \quad (4)$$

Note that *C* is the crucible mass, [g] + sample mass before subjecting to heating, [g], G is the crucible mass, [g] + sample mass after the heating process, [g], H is the mass of the crucible (empty) and $M._C$ is wetness content, [%]. and $V._M$ is the volatile percentage by mass wetness amount, [%].

Ash content determination: When the volatile material was removed, 181.15g of the sample was put into a known-weight crucible. It was heated to 700 °C for 3hr in a muffle furnace. The crucible was left open as it heated up. Following the necessary heating, the crucible was cooled to room temperature in a desiccator, at which point the weight of the ash was measured and noted. Equation 5 is used to get the percentage ash content.

$$A.c = \frac{100(G - H)}{C - H} \quad (5)$$

Note that *C* is the crucible mass, [g] + sample mass before subjecting to heating, [g], G is the crucible mass, [g] + sample mass after the heating process, [g], H is the mass of the crucible (empty) and $A._c$ is the percentage wetness amount, [%].

Fixed carbon content determination: Fix carbon amount percentage was mathematically obtained using modelled equation 6.

$$\text{Fixed carbon amount } (F._C) = 100 - (\%M._c + \%\ V._c + \%\ A._c) \quad (6)$$

SEM Analysis Studies: Using a SEM instrument, the microstructural as well as the surface of the RS-AC were analyzed (model HITACHI, S-3400N). The SEM stubs were mounted with the AC powder (layered with sticky carbon tape). The stub was then put into an EMITECH K550X sputter coater for five min to receive a gold coating to offer high reflectivity during the scanning process.

F-T-IR analysis studies: The IPRrestige-21, F-T-IR-84005, and SHIMADZU Corporation were used for the FTIR analysis (Kyoto, Japan). Spectroscopy grade KBr (Merk, Darmstadt, Germany) and 0.1g of RS-AC sample were combined in a mortar. A portion of this mixture was added to a cell with a hydraulic pump piston connected, creating a compression pressure of 15kPa/cm^2. To avoid interfering with any oxides of carbon or vaporized moisture, the mixture then transformed into a solid disc and baked at 105°C for 4hr. It was then transported to the Fourier transformed-IR-analyzer, where a tallying chromatogram signal produced, revealing the λ of sample's respective reactive groups in the sample that had been known by contrast between text values and those obtained in the laboratory.

2.5 Adsorption Study

Adsorption parameters like contact duration, temperature, and bio-adsorbent dosage were changed during the process to examine the efficacy of RS-AC for pollutants removal away from the chosen wastewater sample obtained from abattoir.

Effect of contact period: Using 0.6g of RS-AC to touch 50ml of abattoir effluent sample and placed on a water bath shaker for parameter variables of 10min, 200rpm as well as at same temperature value of 60^{o}C for which the impact of contact duration was investigated. The resultant mixture was filtered, yielding treated water as the filtrate and the bio-adsorbent as a residue. The technique was assessed throughout a time span of 10 to 60min, with 10min intervals.

Effect of temperature: A dosage of 0.6g of bio-adsorbent was added to 50ml of the waste water from an abattoir, and the mixture was then water bathed using shaker set at 20^{o}C with continual contact period set to 60min. between respective temperatures varying from 40, 60, 80 as well as 100^{o}C, the process was repeated.

Effect of RS-AC dosage: At 80°C, potential hydrogen level 5, 50ml of abattoir effluent sample at 200rpm, and 60 min of contact period, the effect of dosage was evaluated. 50cc of abattoir wastewater were heated at 80ºC with 0.1g of the RS-AC added. To separate the residue from the filtrate, the mixture was agitated at 200rpm and filtered. With a 0.1g gap experimental repetition from 0.2 through 0.6g.

2.6 Treated Samples Heavy Metal Determination

The potential chemically modified samples were studied to ascertain the content of Fe ions as well as COD-limit retained after modification at the changing experimental variables.

2.7 Adsorption Kinetic Studies

At the same time interval as the effect of contact, the PFOKM and SOKM were studied.

Pseudo-first-order kinetic model (PFOKM): Lagergren illustrated fluid strong stage adsorption frameworks to illustrate the first-request rate condition, which is the most precisely realized one. Lagergren's model has been referred to as PFOKM equation to differentiate energy conditions reliant basis of centralizations away from adsorption limitations of solute materials (Smith *et al.*, 2011).

$$\frac{dR_s}{ds} = L_{1p}(R_e - R_s) \quad (7)$$

where L is the rate constant of the pseudo first-order adsorption, [1/min], on integration with the boundary conditions from s=0 to s=s and from R_s=0 to R_s = R_s develops equation 8.

$$ln\,[\frac{R_s}{R_s - R_s}] = L_{1p}s \quad (8)$$

SOKM: This mathematical model order, as described in equation 9 which discusses the rate at which the level of COD was reduced as well as the Fe adsorption with respect to time and adsorption rate with regards to reaction sites.

$$\frac{dr}{ds} = l_2(r_e - r_s)^2$$
(9)

l_2 is the SOKM constant with regards to the rate of the process, showed linear progress as in Equation 10.

$$\frac{s}{r_s} = \frac{1}{l_2 r_e^2} + \frac{s}{r_e}$$
(10)

A graphical trace of $\frac{s}{r_s}$ versus s results a linear plot for the SOKM.

Exponential form of the equation gives the Elovich kinetic model (EKM) as modelled in equation 11.

$$\frac{dC_s}{ds} = \alpha.\exp(-\beta C_{.s}) \quad (11)$$

α and β are the EKM-constants. α depicts the bio-absorption difference as time changes β shows the surface rate change. $C_{.s}$ is central bio-adsorbate towards limiting level at time (s).

2.8 Models for the Bio-adsorption Process

Bio-adsorption balances are set of circumstances where quantities of particles hitting the adsorbent-bio-surface equals quantity of ions or atoms disappearing. The adsorption isotherm represents the interconnection between the quantity of substance taken up by a strong take up bio-sorbent as well as the substance's balance convergence at constant temperature (Osibanjo & Adie, 2007).

The Freundlich-Langmuir isotherms are utilized for ascertaining the isotherm for modelling the adsorption processes. By deciding on the distinguishing relationship coefficients (R_2), the workability of the modelled isotherm condition to the conducted-adsorption investigations were taken into consideration (Tan *et al.*, 2008).

Langmuir-modelled isotherm: This modelled-isotherm depicts bio-sorbent frameworks with a maximum inclusion of one subatomic layer for the adsorbate. Notwithstanding the fact that Langmuir's initial isotherm proposal (1918). According to the Langmuir model, a single particle has a single surface site, the surface is homogeneous, and adsorption is restricted to that site for each adsorbate atom (Altin *et al.*, 1998). Linear type Langmuir-modelled isotherm criteria with straight type is defined as depicted in equation 12.

$$\frac{de}{Re} = \frac{1.0}{R_o K_l} + \frac{1.0}{R_o}\ de \tag{12}$$

Note that d_e, [mg/g] represent the highest quantity taken-up and R_e[L/mg] is dosage adsorbed with respect to time, correspondingly, and R_o and K_l are constants connected to Langmuir-modelled isotherm linked to bio-adsorbent's one-layered adsorption. A dimensionless equilibrium parameter can be used to express the key features of Langmuir-modelled isotherm labelled R_L. This variable's definition is defined as in equation 13 (Tan *et al.*, 2008).

$$\frac{1.0}{K_L C_O + 1} = R_L \tag{13}$$

$1<R_L$ 1 is un-favourable, $1=R_L$ linear, $0.0<R_L<1.0$ is favourable and $0=R_L$ is irreversible.

Freundlich-modelled isotherm: The depiction of organics matters being absorbed from fluids to carbonic compounds heavily utilizes Freundlich-modelled isotherm condition (Foo and Hameed, 2010). This condition requires the supporting structure depicted in equation 14.

$$(P^{1/n})K = C \tag{14}$$

Writing the Freundlich- modelled isotherm in natural logarithm notation gives birth to equation 14.

$$\frac{1}{n}\log C_e + \ logK_f = \mathrm{Log}Q_e \tag{15}$$

K_f as well as n represents the Freundlich-modelled iso-constants as n signifying agreement with the bio-sorption trend. K_f is the coefficient of distributed sample and depicts the extent of bio-sorption.

3. Results-obtained and Discussion

3.1 Proximate-analyses

Proximate-analytical study was used to ascertain the sample's wetness, volatile, and ash contents as well as the amount of remaining carbon. The wetness content of the precursor is shown in Table 1. The precursor had a 5.00% wetness content, 4.66% volatile matter content, 3.80% ash percentage, and 87.14% carbon content. The precursor can be used as a high yield source for AC because of the precursor's high carbon content. The sample's wetness content reveals that it is porous and that it has the right amount of wetness. The sample's adsorptive ability has been found to increase with decreasing wetness content (Minelli *et al.*, 2002). Ash concentration typically reveals the inorganic components linked to carbon. Higher carbonization temperatures are thought to increase the precursor's ash content since they tend to reduce the volatile stuff in bio-adsorbents.

Table 1 - Proximate analytical studies of the (RS)-Precursor.

Parameters / %	RS/×10
$M_{.C}$	0.5
$V_{.M}$	0.4
$A_{.C}$	0.3
$F_{.C}$	8.7

3.2 Bulk-Density

In this studies, bulk-density of the sample was calculated using dried content basis (see Table 2). Bulk density provides a clue as to the bio-adsorbent's ability to float. It implies that adding AC to water will cause it to sink, resulting in better contact with the adsorbate and an efficient bio-adsorption process. The bulk density of the sample is displayed in Table 2. The sample (pyrolysis at 400^0C) has a bulk density of 0.42g/cm, as can be shown. ACs are often thought to be suitable for adsorption when their bulk density ranges from 0.3 to 0.5g/cm3 (Tariq *et al.*, 2023).

Table 3- RS-AC Properties gotten

Variables	RS-AC/×10
potential hydrogen level	0.50
% produced yield	9.53
% burn-Off	0.47
Density(bulk) / gcm^{-3}	0.04

3.3 Effect of contact period

Using 0.6g of the bio-adsorbent, 50ml of abattoir effluent sample, potential hydrogen level of 5, 200rpm with fixed heat level 60^oC, impact of contact duration was investigated. evaluated between 10 and 60min. (Figure 1) illustrates how the adsorption effectiveness for Fe and COD grew with time. With a maximum adsorption efficiency of 99.198%, Fe content decreased from 0.374×10^2mg/L to 0.003×10^2mg/L. The recorded level of bio-sorption was highest at 70.265%, and the limit of COD-limit content was also lowered from 854mg/L to 250mg/L.

3.4 Effect of temperature

Using 0.6g of the bio-adsorbent, a potential hydrogen level of 5, 50ml of abattoir effluent sample, 200rpm, and 60 min of contact period, the impact of temperature was investigated. evaluated between 20 and 100^oC in temperature. (Figure 2) illustrates how the temperature increased the adsorption effectiveness for Fe and COD. With a maximum adsorption effectiveness of 99.465%, the amount of iron decreased from 37.4mg/L to 0.2mg/L. The greatest adsorption efficiency was 74.239%, and the COD concentration decreased from 854mg/L to 220mg/L.

3.5 Effect of dosage

At 80ºC, potential hydrogen level 5, 50ml of abattoir effluent sample, 200rpm, and 60min of contact period, the effect of dosage was investigated. 0.1 to 0.6g of dose were evaluated. Once the dosage was raised, the effectiveness of iron and COD adsorption improved, as shown in (Figure 3). The greatest adsorption effectiveness was 96.52406%, resulting in a reduction in iron concentration from 37.4mg/L to 1.3mg/L. The maximum adsorption efficiency was 67.21311%, and the COD content decreased from 854mg/L to 309mg/L. The saturation of the bio-adsorbent's pore spaces is what causes the reduction in the amount of Fe and COD adsorbed.

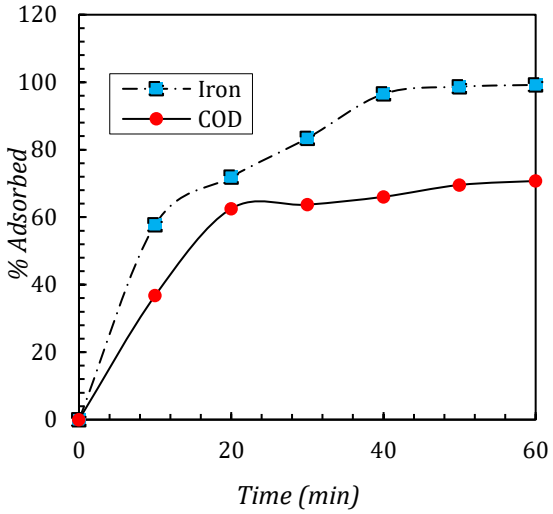

Figure 1 -Contact period effect

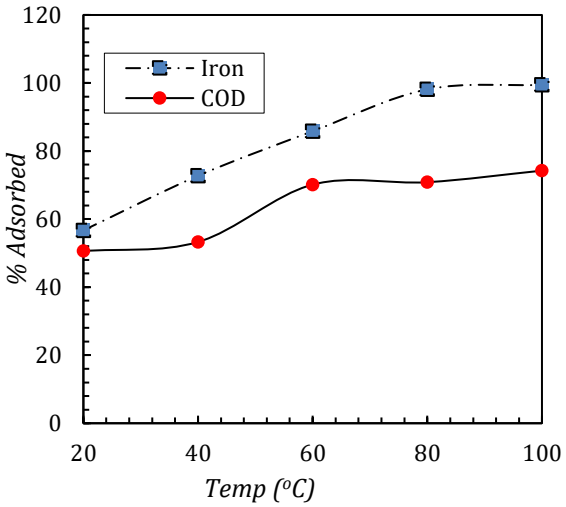

Figure 2 -Effect of temperature.

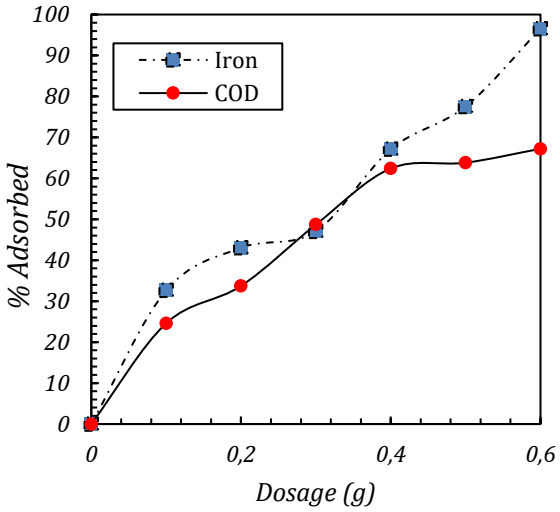

Figure 3 –Dosage increment effect

3.6 Isotherms of the Adsorption

Various models developed explain the correlation for the amount absorbed by the bio-adsorbent at equilibrium and the dose still present.

Figures 4 through 7 shows the studied isotherms for Fe as well as COD in respective order. These diagrams correspond to a straight-line equation, as equations 11 through 14 are used to know the isotherm parameters, shown from analysing coefficients side by side, Langmuir-model happens to be most fitted straight lined mathematics model that best describes COD-limits reduction as well as Fe dosage within (0.7155) which is more realistically accepted compared to standard. The R_L found

for the adsorption of COD is 2.251957, indicating the adsorption was not favourable for COD (which is greater than 0). R_L of 7.5×10^{-2} is best for Fe dose reduction in the solution. The adsorption was advantageous for iron (which is greater than 0, but less than 1). The Freundlich isotherm model, whose correlation coefficient was larger (0.8771) than that of the Langmuir isotherm (0.4824), was also shown to be more befitting for Fe dosage reduction from comparing the coefficient of correlations.

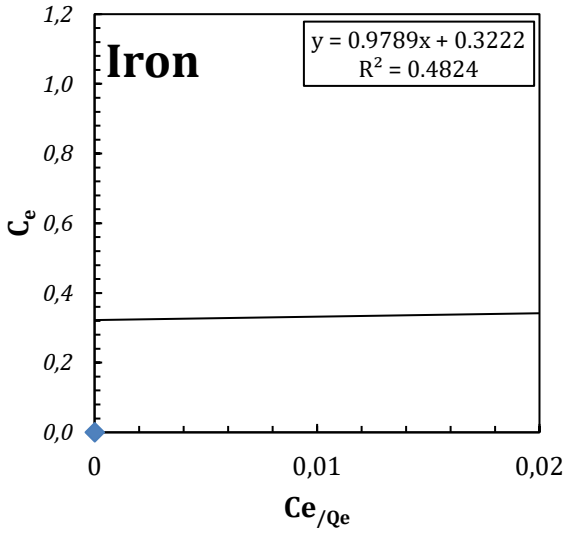

Figure 4 - Langmuir isotherm for iron.

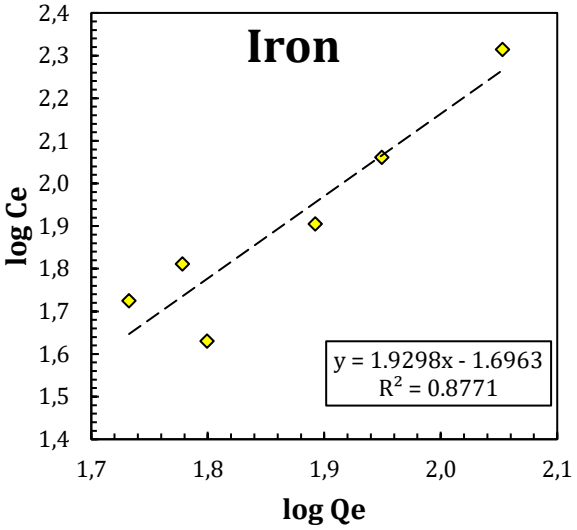

Figure 5 - Freundlich isotherm for iron adsorption.

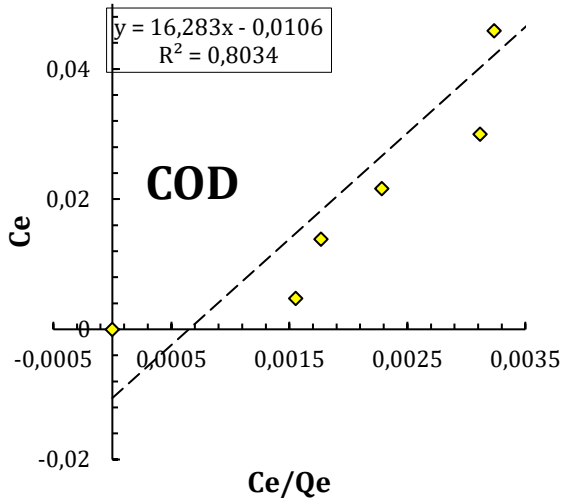

Figure 6 - Langmuir isotherm for COD.

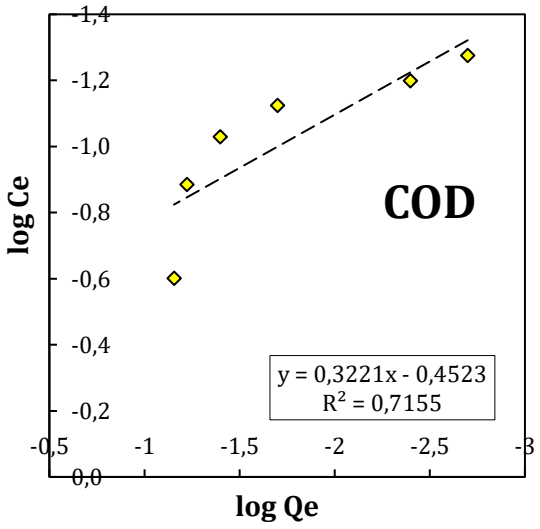

Figure 7- Freundlich isotherm for COD adsorption.

3.7 Adsorption kinetics

The first-order model is the model that best fits the solute-solvent movement. Equations 7 and 8 provide the model's linear form. The models for iron and COD are shown in Figures 8 and 9. R_2 of 95.43×10^{-2} for Fe and $0.44.02\times10^{-2}$ for COD-limits had a lower regression correlation than a SOKM. Therefore, from inference the SOKM is best fit model.

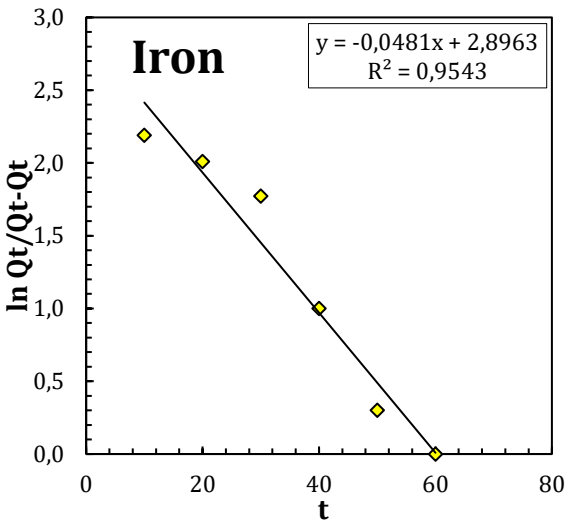

Figure 8 - PFOKM for Fe-adsorption.

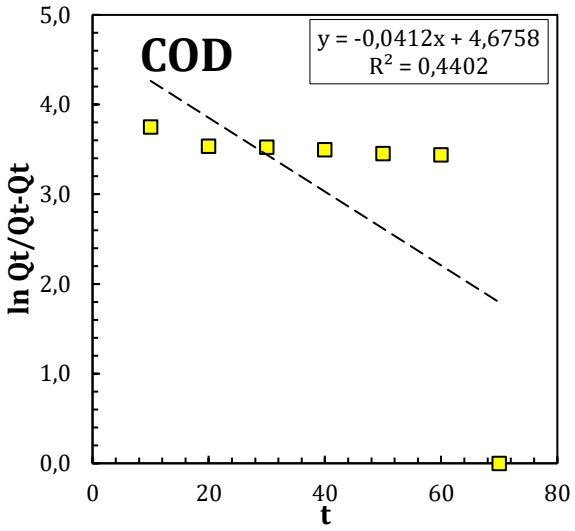

Figure 9 - PFOKM for COD adsorption.

Equation 2.4 is used to define the SOKM rate, as shown in Figures 10 and 11 for respective variables under consideration, R_2 values of 99.36×10^{-2} and 98.9×10^{-2} for each were gotten. As a result, the SOKM, which has higher correlations than the first order model, fits the data currently available for both iron and COD adsorption.

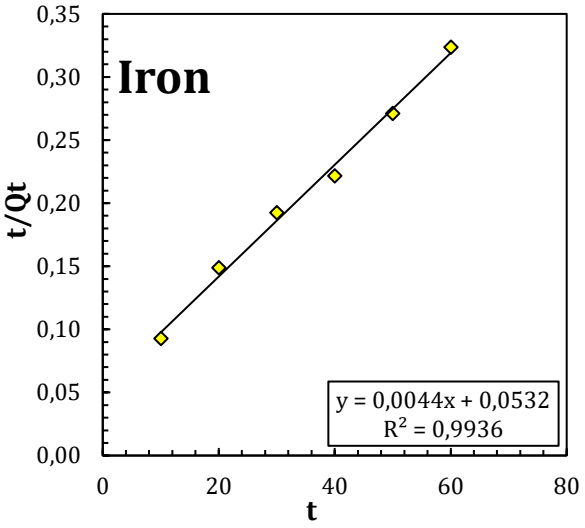

Figure 10 - SOKM for iron adsorption.

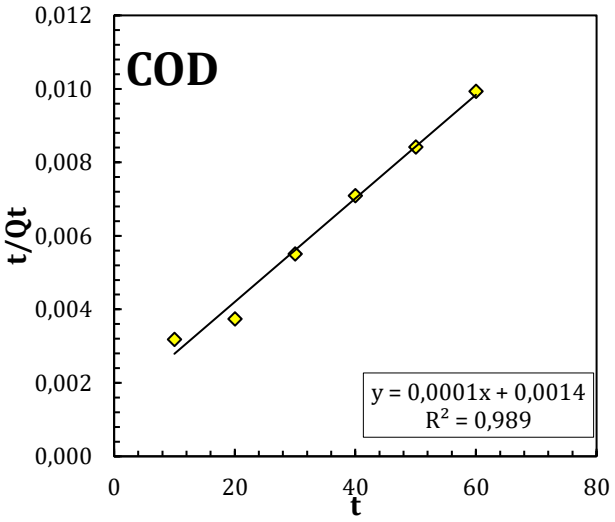

Figure 11 - SOKM for COD adsorption.

The iron and COD data from the current work did not suit the Elovich's model well. According to Figures 12 and 13, the R_2 values for iron and COD are 0.9724 and 0.8597, respectively. Based on the findings of the kinetic investigation, inferring the second-ordered formed model for the kinetics analysis best describes how iron and COD adsorb to the precursor in the current study. The SOKM postulates that "chemical adsorptions," which include creating valence amongst bio-adsorbents as well as adsorbates there by controlling the bio-adsorption process (Xu and Wan, 2017).

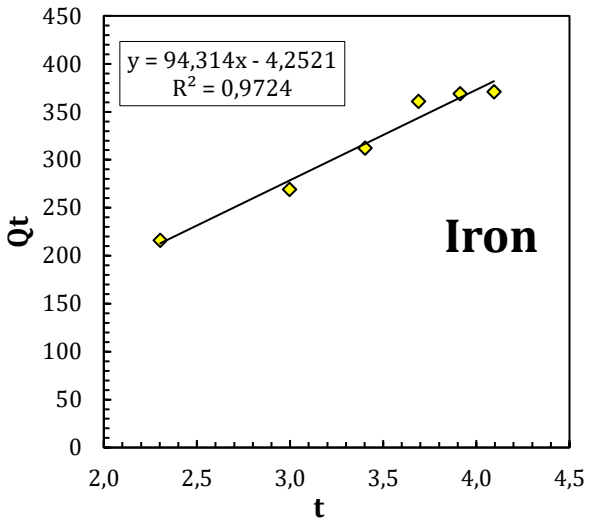

Figure 12- Elovic kinetic model for iron adsorption.

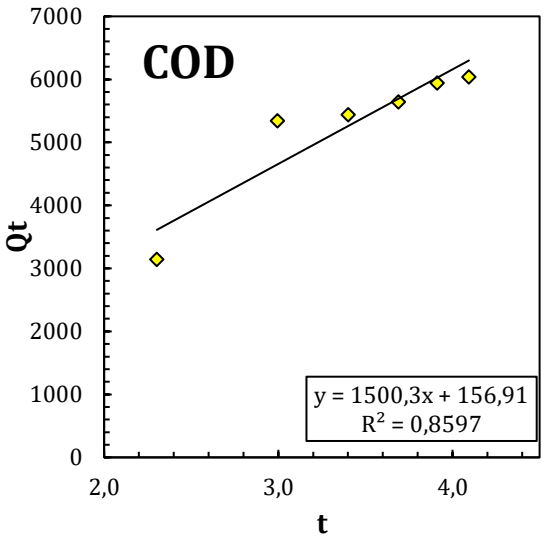

Figure 13 - Elovic kinetic model for COD adsorption.

3.8 Structural analysis by Scan Electron Microscope (SEM)

Figure 14 shows the RS-AC SEM image at 500x, 1000x, and 1500x. The material is porous and crowded, as seen in the SEM image. The elemental makeup of the RS-AC is displayed in Table 3 based on the results of the SEM-EDS investigation. The presence of C, Si, and O atoms in RS-AC contributes to the material's strong capacity to form pores, layers, and linkages with the substances it absorbs.

Table 3- Elements of the RS-AC

Element Number	Element Symbol	Element Name	Atomic Conc.	Weight Conc.
6	C	Carbon	67.69	49.78
14	Si	Silicon	20.81	35.79
8	O	Oxygen	7.73	7.57
15	P	Phosphorus	0.96	1.82
13	Al	Aluminum	0.52	0.85
19	K	Potassium	0.35	0.85
30	Zn	Zinc	0.21	0.83
16	S	Sulfur	0.37	0.73
7	N	Nitrogen	0.75	0.64
12	Mg	Magnesium	0.29	0.44
17	Cl	Chlorine	0.21	0.27
11	Na	Sodium	0.12	0.17

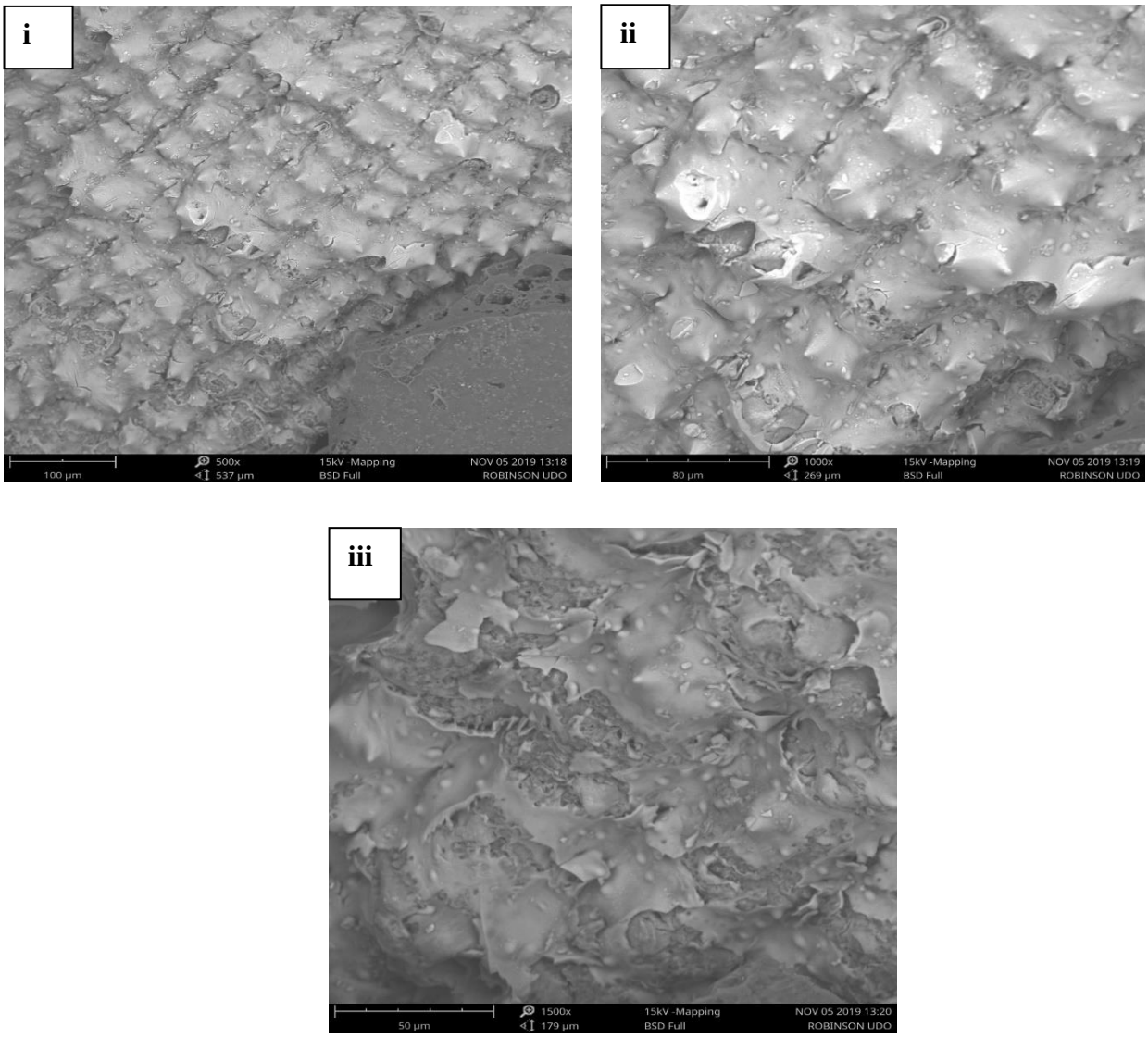

Figure 14 – SEM-Images of RS-AC at (i) $5x10^2$x-magnification (ii) $10x10^2$x-magnification (iii)$15x10^2$x-magnification

3.9 Fourier-Transform-Infrared F-T-IR

Spectra of the F-T-IR, as displayed in Figure 15, allowed for identification of the principal chemical groups present in the RS-AC. The wide band between 2700cm^{-1} and 4000cm^{-1} was used to represent the silanol OH groups and adsorbed water. Siloxane bonds cause the main absorbance peak at 1200cm^{-1} (Si-O-Si). The siloxane network's vibration nodes are shown as peaks between 900 cm^{-1} and 1000 cm^{-1}. Then, Figure 15 further demonstrates the strong adsorption bands relating towards OH-vibrations of adsorbed H_2O, disturbed silanols, as well as free silanols surface at 3700 cm^{-1} to 3700 cm^{-1}.

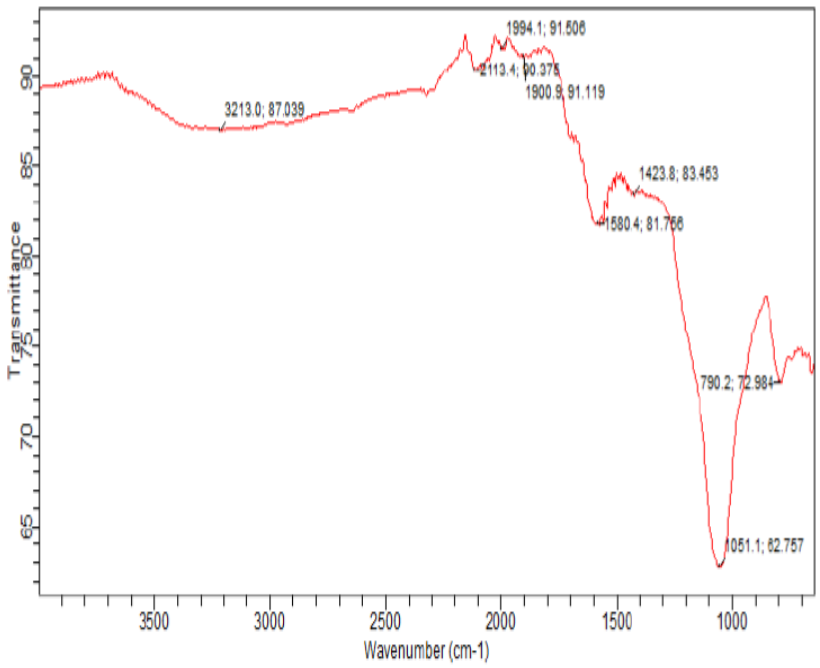

Figure 15 –Fourier-Transform-Infrared (F-T-IR).

4. Conclusion

Phosphoric acid was used to create activated carbon using RS as a precursor. Several characterization methods, including proximate, density (bulk), SEM, and F-T-IR, were considered in the study. A subsequent adsorption experiment is conducted to reduce the iron and COD levels and limits correspondingly in the abattoir wastewater to acceptable levels. The adsorbent underwent a sample SEM examination, which revealed the adsorbent's pore structure. The current investigation shows that the generated RS-AC can be effectively used to keep the level of Fe and COD-limit in aqueous solution to acceptable standards and may be used for water as well as effluent and industrial discharge treatments, according to the study done on RS-AC. According to this research, RSAC has a high fixed carbon content, which makes it an effective adsorbent as well as the obtained RSAC's bulk density is suitable for maintaining flow constancy. The F-IM best matches the linear equation for iron removal, while the L-IM has a correlation coefficient that best fits the linear equation to maintain COD limit levels to standard.

Additionally, comparison to the other models, the second order kinetic model best fits the current data to keep the COD and iron levels within acceptable ranges. Conclusively, the process is controlled by Chemical adsorptions.

Acknowledgements
The authors appreciate the support from The Federal University of Technology Minna, Nigeria.

References

Adeyemi, I. G., & Adeyemo, O. K. (2007). Waste management practices at the Bodija abattoir, Nigeria. *International Journal of Environmental Studies*, 64(1), 71-82. https://doi.org/10.1080/00207230601124989

Altın, O., Özbelge, H. Ö., & Doğu, T. (1998). Use of general-purpose adsorption isotherms for heavy metal–clay mineral interactions. *Journal of colloid and interface science*, *198*(1), 130- 140. https://doi.org/10.1006/jcis.1997.5246

Aniyikaiye, T. E., Oluseyi, T., Odiyo, J. O., & Edokpayi, J. N. (2019). Potential hydrogen levelysico-chemical analysis of wastewater discharge from selected paint industries in Lagos, Nigeria. *International journal of Environmental Research and Public Health*, *16*(7), 1235. https://doi.org/10.3390/ijerpotential hydrogen level16071235

El-Shafey, E.I. (2005). Behaviour of Reduction–Adsorption of Chromium (VI) from an Aqueous Solution on a Modified Sorbent from Rice Shell, Water, Air, Soil Poll. *Journal Bio-resource Technology*. 163, 81–102

Foo, K. Y., & Hameed, B. H. (2010). Detoxification of pesticide waste via activated carbon bio- adsorption process. *Journal of hazardous materials*, *175*(1-3),1-11. https://doi.org/10.1016/j.jhazmat.2009.10.014

Mekuria, D. M., Kassegne, A. B., & Asfaw, S. L. (2021). Assessing pollution profiles along Little Akaki River receiving municipal and industrial wastewaters, Central Ethiopia: Implications for environmental and public health safety. *Heliyon*, *7*(7), e07526. https://doi.org/10.1016/j.heliyon.2021.e07526

Minelli, M., Baschetti, M. G., Doghieri, F., Ankerfors, M., Lindström, T., Siró, I., & Plackett, D. (2010). Investigation of mass transport properties of microfibrillated cellulose (MFC) film. *Journal of Membrane Science*, 358(1-2), 67-75. https://doi.org/10.1016/j.memsci.2010.04.030

Osibanjo, O & Adie, G. U. (2007). Impact of effluent from Bodija abattoir on the potential hydrogen levelysiochemical parameters of Oshunkaye stream in Ibadan City, Nigeria." *African Journal of Biotechnology*, 6(15). https://doi.org/10.5897//AJB2007.000-2266

Smith, W. A., Zhang, N., & Hu, W. (2011). Hydraulically interconnected vehicle suspension: handling performance." *Vehicle System Dynamics*, 49(1-2), 87-106. https://doi.org/10.1080/004231110035963

Sugashini, S. & Mile, S. (2013). Studies on the Performance of Ethylamine- Modified Chitosan Carbonized Rice Shell Composite Beads for Adsorption of Metal Ion, *Journal of Bio-resource Technology*. 17, 97–106.

Tan, I. A. W., Ahmad, A. L., & Hameed, B. H. (2008). Adsorption of basic dye on high-surface-area activated carbon prepared from coconut husk: Equilibrium, kinetic and thermodynamic studies. *Journal of hazardous materials*, *154*(1-3), 337-346. https://doi.org/10.1016/j.jhazmat.2007.10.031

Tariq, W., Arslan, C., Tayyab, N., Rashid, H., & Nasir, A. (2023). Application of agro-based bio- adsorbent for removal of heavy metals. In *Emerging Techniques for Treatment of Toxic Metals from Wastewater* (pp. 157-182). Elsevier. https://doi.org/10.1016/B978-0-12-822880- 7.00008-X

Vassileva, P., Detcheva, A., Uzunov, I. & Uzunova, S. (2015). Removal of Metal Ions from Aqueous Solutions using Pyrolyzed Rice Shells: Adsorption Kinetics and Equilibria. *Journal of Environmental Science*. 42, 4462–.4471

Xu, L., & Wang, J. (2017). The application of graphene-based materials for the removal of heavy metals and radionuclides from water and wastewater. *Critical Reviews in Environmental Science and Technology*, *47*(12), 1042-1105. https://doi.org/10.1080/10643389.2017.1342514

Zhang, B., Zhang, L., & Zhang, X. (2019). Bioremediation of petroleum hydrocarbon-contaminated soil by petroleum-degrading bacteria immobilized on biochar. *RSC advances*, *9*(60), 35304-35311. https://doi.org/10.1039/C9RA06726D